Synthesis of an Antenna System with Frequency Scanning

Islam J. Islamov, Murad M. Jahangirov, Namik M. Shukurov, Simnara R. Ahmadova

Abstract – **The paper proposes a method for synthesizing an antenna system. The proposed technique makes it possible to find the required amplitude-phase distribution in a relatively short time (seconds). With the help of the proposed technique, it is possible to evaluate the potential capabilities of the antenna during adaptation, taking into account mutual connections. The developed algorithm can synthesize optimal solutions for antenna arrays with the proposed objective function aimed at maintaining the width of the main lobe of the full antenna array after its rarefaction and minimizing the peak level of side lobes. With a symmetrical edge type of rarefaction, it is possible to reach the values of the peak level of the side lobes faster than with other types. When the antenna array is rarefied by more than half, the differences between the used amplitude distributions of the field over the aperture of the full array are minimized.**

Keywords – **Antenna System, Synthesis, Frequency Scanning, Amplitude-phase distribution, Directional Action, Diagram.**

I. INTRODUCTION

On-board antennas for small and ultra-small aircraft are subject to requirements related to overall dimensions and placement features. At the same time, since the functionality of the antenna-feeder system will deteriorate, the aim is to make the best use of the antenna elements. In some cases, it is necessary to combine emitters placed in randomly selected places of the carrier into an antenna array.

The paper considers three-dimensional antenna arrays [1], the mutual position of the elements of which is fixed. If the radiating elements are located on any surface, then such antenna arrays are called surfaces according to the standard [2]. But, traditionally [3], the term conformal antenna array is used.

The modern development of wireless broadband access systems has led to an increase in the ranges allocated for these systems, the development and implementation of complex antenna systems and appropriate signal processing methods. In this regard, there are increased requirements for terminal equipment, in particular antenna systems.

Therefore, the use of efficient antennas with good weight, size and electrodynamic characteristics will significantly expand the frequency ranges and coverage of services, as well as increase their throughput. To solve this problem, it is necessary to use antenna systems based on antenna arrays and radiators operating in a wide frequency band and having sufficient gain and directivity.

Article history: Received December 02, 2022; Accepted May 29, 2023

Islam J. Islamov, Murad M. Jahangirov, Namik M. Shukurov, and Simnara R. Ahmadova are with the Department of Radio Engineering and Telecommunication, Azerbaijan Technical University, H. Javid ave. 25, AZ1073, Baku, Azerbaijan, E-mail: icislamov@mail.ru

These criteria include antenna arrays with an arbitrary arrangement of radiating elements, which have good electrodynamic characteristics in the frequency band allocated for wireless broadband access systems.

Antenna arrays with an arbitrary arrangement of radiating elements - a broadband directional antenna operating in a tenfold or more wide wavelength range. In terms of gain, the antenna is equivalent to a five-element "wave channel" type antenna and consists of a number of vibrators connected to a two-wire line with a serial polarity reversal of the vibrator feed points, the lengths of which and the distances between them decrease exponentially in the direction to the feeder connection points. Behind the longest vibrator, a short-circuit jumper is installed, which improves the matching of the antenna with the feeder and provides balancing. For the synthesis of antenna arrays with an arbitrary arrangement of radiating elements, it is necessary to calculate the radiation pattern, input impedance, standing wave coefficient and directivity. The shape of the radiation patterns completely determines the most important energy characteristic of the antenna - the directional coefficient.

The main advantages of cylindrical antenna arrays with an arbitrary arrangement of radiating elements are: the possibility of wide-angle (up to 360°) scanning by a beam of constant width and shape in the azimuthal plane (in the plane of the arc); scanning in elevation plane (up to ±50°); weak in comparison with flat and linear antenna arrays, the mutual connection of emitters due to the spatial rotation of their axes; constructive convenience of placing convex antenna arrays on a number of objects.

Thus, the use of antenna arrays with an arbitrary arrangement of radiating elements will make it possible to form several beams of radiation patterns with appropriate sectorization and significantly expand the coverage area due to the high directivity in all directions, increasing the capacity of the system as a whole, and increase the throughput and energy of the terminal equipment.

Recently, in connection with the creation of multifunctional radio-electronic means for various purposes and the significant complication of the radio-electronic environment, the use and placement of phased antenna arrays, which provide a solution to a wide range of tasks on carrier objects, have become particularly relevant. Flat antenna arrays with an aperture with an arbitrary shape of the boundary are widely used, which is due to the need to place apertures of various ranges on a limited area of the surface allocated for antenna systems. These situations arise when antennas are installed on ships, cars, etc. Another feature associated with the need to operate phased antenna arrays in a complex interference environment is the formation of radiation patterns with an arbitrary law of change in the level of side lobes, including a low level.

Antennas with electrically controlled phase distribution provide beam scanning in space at a speed that can be several orders of magnitude higher than the speed of mechanically scanning antennas. The installation time of a phased array beam at a given point in space is practically determined by the speed of the electric phase shifter or frequency tuning during frequency scanning and is not related to the weight and dimensions of the antenna. Phased antenna arrays of highly directional antennas allow you to increase the maximum realizable resolution, gain and maximum power of the antenna. Arrays make it possible to create multifunctional antennas in which, with the help of electrically controlled microwave devices, the shape and width of the radiation pattern change depending on the functions performed by the radio system.

In the well-known literature, for example, [1, 3], as a rule, recommendations are given on the formation of an arbitrary law of change and reduction of side lobes for a phased antenna array with a canonical opening shape (rectangular and round openings). For such openings, the relationship between the opening parameters (opening size, the law of change in the amplitude distribution in the opening) with the width of the main maximum of the radiation patterns and the law of changing the level of side lobes have been well studied. At the same time, these regularities refer to the case of using the row-column control law for the amplitude-phase distribution in rectangular openings or axisymmetric distribution in round openings.

However, in the case of openings with an arbitrary shape of the boundary, the use of a phased antenna array construction scheme that implements, for example, a row-column control law for the amplitude-phase distribution, can lead to inaccurate installation of the main beam, as well as to a significant increase in the level of side lobes. These shortcomings are due to the refusal to take into account the shape of the aperture when using the row-column control law for the amplitude-phase distribution. In addition, in the known literature, there are no results of studies of the relationship between the parameters of the radiating aperture and the generated radiation patterns.

In connection with the foregoing, an important task is to consider the algorithm for the synthesis of the amplitude-phase distribution for a phased antenna array with an arbitrary shape of the boundary.

One of the ways to solve the problem is to introduce an equivalent flat aperture with a canonical boundary shape, in particular, rectangular, round, etc., in which the real aperture of a phased array antenna fits in the best way.

II. METHODS

A feature of the antenna array is the presence of mutual connections between the radiating elements. The main mechanism for the emergence of a mutual connection between the radiating elements of the array is associated with the scattering of the field of each element by the rest. It is noted in [4] that the field scattered from the antenna system is divided into two components:

- re-reflections from an unmatched load (thus, a connection of the reflected field with the antenna pattern appears);
- diffraction of electromagnetic waves on the elements of the antenna structure.

From the point of view of the general theory of microwave circuits [5], the antenna array can be associated with the scattering matrix *S*, which, due to mutual connections, has an off-diagonal form. The matrix S relates the incident and reflected waves. The incident waves are directed towards the multipole and in the case of an antenna array are mainly determined by the sources of electromagnetic waves (generators) connected to the array. Reflected waves are waves coming from the antenna array, i.e. waves directly reflected from the inputs of the array, and waves coming from other generators due to mutual connections.

The reflected waves are involved in the formation of the antenna array radiation patterns only in the case of their reflection from the mismatched outputs of the generators when they change direction and turn into incident ones. As a result, it turns out that the excitation of the antenna array or the amplitude-phase distribution is formed not only due to the primary incident waves from the generators but also due to the reflection of the reflected waves from the generators. The full amplitude-phase distribution is their sum.

The situation becomes more complicated if, when the amplitude-phase distribution changes, the load resistances of the radiating elements change. For example, when the state of industrial phase shifters changes, not only the phase changes but also their input and output resistances. We will assume that the functional elements [6] that provide excitation of the antenna array are devices, the input the resistance of which does not change with a change in the excitation of the lattice. Such an assumption is quite appropriate for modern arrays - active phased antenna arrays, including digital ones.

It was shown in [7] that to eliminate the negative effect of mutual impedance, it is necessary to introduce pre-distortion into the initial current distribution, which compensates for the effect of the mutual influence of emitters. As a result, the ideal current distribution in all calculations must be replaced by a distorted distribution.

In real antenna arrays, there is a spread of parameters associated with the inaccuracy in the manufacture of microwave path nodes and the deviation of material characteristics from the specified ones. Therefore, each grating goes through a calibration and adjustment procedure [8], which, in particular, reduces the negative effect of mutual connections. As a result, a one-to-one correspondence is found between the amplitude-phase distribution formed at the outputs of the generators and the required amplitude-phase distribution at the inputs of the emitters.

Further, we will consider such antenna arrays for which either the tuning and calibration procedure was carried out, or pre-distortions were introduced into the original amplitude-phase distribution. Usually, they try to make the feeder path of the array consistent with the radiating elements, so the distortion of the amplitude-phase distribution in some cases can be neglected. For example, if the output of the transceiver module closest to the antenna contains a ferrite product (circulator or valve), then the radiating elements will always be loaded with a matched load. In this case, the main role will be played by the diffraction of electromagnetic waves on the structural elements of the antenna, including neighboring radiating elements.

To take into account the diffraction component of the mutual influence of radiating elements, the method of partial diagrams is used. The apparent ambiguity of this term should be noted. The word “partial” means “partial, part of something”. In fact, any representation of a field as a sum of several fields is a decomposition into partial components. Since there can be several variants of such a decomposition, clarifications are needed. Here are some examples from contemporary sources.

In [9], it is noted that, since there is always an electromagnetic interaction between the elements of the array, the radiation corresponding to the excitation of one input, strictly speaking, is formed by all its elements, and therefore the radiation pattern of an element is called a partial radiation pattern. All radiating elements are excited in turn, while the remaining elements are loaded on matched loads. To form the required radiation patterns, it is necessary to find the corresponding amplitude-phase distribution, multiply it by the partial fields, and then add them. With this representation method, the number of partial radiation patterns coincides with the number of elements in the array.

In [10], the number of parts diagrams can be either less or more than the number of emitters. A linear equidistant antenna array is considered. The partial is the radiation pattern generated by all radiating elements with equal amplitude excitation with a linear phase shift. That is, the partial fields described earlier in [9] are multiplied by the amplitude-phase distribution of the indicated type and added. In this case, to form the required radiation patterns, it is necessary to find the appropriate weighting coefficients, multiply them by partial fields, and then add the already weighted fields. The resulting amplitude-phase distribution will be equal to the sum of the amplitude-phase distribution of partial radiation patterns, each of which is multiplied by the found weight coefficient.

The specific value of the amplitude-phase distribution element is determined by the following formula:

$$Ii_n = \sum_{m=1}^{M} a_m \cdot Iip_{nm}, \tag{1}$$

where Ii (Ii_1, Ii_2,…,Ii_n,…,Ii_N) – is the resulting amplitude-phase distribution; N is the number of emitters in the antenna array; $Iipm = (Iip_{1m}, Iip_{2m},\ldots,Iip_{nm},\ldots,Iip_{Nm})$; $m = 1\ldots M$ – amplitude-phase distribution of partial radiation patterns, equal amplitude with linear phase shift; M is the number of partial radiation patterns; $A = (a_1, a_2,\ldots, a_m,\ldots,a_M)$ weight coefficients.

In the examples presented, the partial radiation patterns are defined differently, but the way in which the interconnections are taken into account is similar. It is necessary to calculate or measure the radiation patterns of the radiator in the array, provided that neighboring radiators are loaded with matched loads.

In what follows, we will use the term “partial” in the sense described in [9], unless otherwise specified. That is, we will mean the field or radiation patterns of the radiating element of the antenna array, taking into account diffraction on the radiators and structural elements of the array. The situation is simplified if we consider equidistant linear antenna arrays in the case when all partial radiation patterns are the same. Then the radiation patterns of the antenna array can be represented as the product of the partial radiation patterns and the array factor [11].

For example, for an equidistant linear antenna array, the radiation patterns can be written as:

$$F(u) = F_0(u)\sum_{n=1}^{N} Ii_n \cdot e^{-i\frac{2\pi(u-1)(n-1)}{N}}, \tag{2}$$

where $F_0(u)$ is the partial radiation pattern; d – the distance between emitters (grid spacing); u – generalized coordinate; $kd\sin\vartheta = 2\pi(1-u)/N$; ϑ is the angle measured from the normal to the antenna array.

The sum in (2) is a lattice factor. The need to write the antenna array radiation patterns in this form is due to the fact that in this case, the array factor coincides with the definition of the MATLAB *fft* function.

The problem of synthesizing radiation patterns is reduced to methods of working with the discrete Fourier transform. When considering signals in the time domain, they pass into the frequency domain; in antenna technology, they move from the region of spatial readings to the angular spectrum [12-14] - from the amplitude-phase distribution to directional patterns.

A feature of the application of digital signal processing methods in antenna arrays compared to signals in the time domain is that we can change not only the amplitude of spatial samples, but also their phase. Although, if the signal is represented as an IQ expansion, then negative frequencies begin to make sense here too. Let's give some examples.

Let's get the amplitude-phase distribution for the formation of sector radiation patterns with a low level of side lobes, shown in Fig. 1.

In fact, the method from [15] was applied, which, follows from the properties of the Fourier transform. Three equal-amplitude amplitude-phase distributions with a linear phase shift are summed term-by-term with weight coefficients, providing a shift of partial (in the sense of [16]) radiation patterns at angles of 20 ($Ii1$), 30 ($Ii2$), and 40 ($Ii3$) degrees from the normal to the antenna. Weight coefficients (1,4; 1,7; 1,0) were obtained by selection. The sum of the weighted amplitude-phase distribution is multiplied by the Chebyshev window to reduce the level of side lobes. It should be noted that the very presence of side lobes is associated with the multiplication of spatial samples by the window. The radiation pattern of a linear equidistant antenna array with equal-amplitude in-phase excitation completely coincides with the spectrum of a rectangular window.

As another example of the use of traditional methods of digital signal processing, we present a method for forming deep zeros in the radiation patterns of an antenna array. For clarity, consider the factor of a linear equidistant array consisting of 64 radiating elements. We take the distance between the emitters four-tenths of the wavelength.

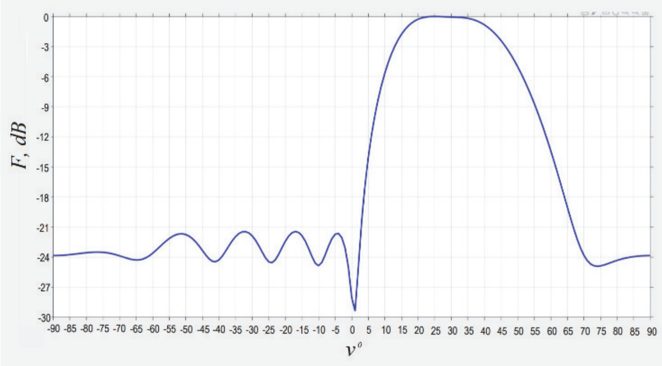

Fig. 1. Amplitude-phase distribution for the formation of sector radiation patterns with a low level of side lobes

The spectrum of a sinusoidal signal is two components symmetrical about zero frequency. Fig. 2 shows the antenna array multiplier and the amplitude-phase distribution that generates it. If we apply a seventh-order Butterworth notch filter to the amplitude distribution, then we will get the grating factor and the corresponding amplitude-phase distribution shown in Fig. 3.

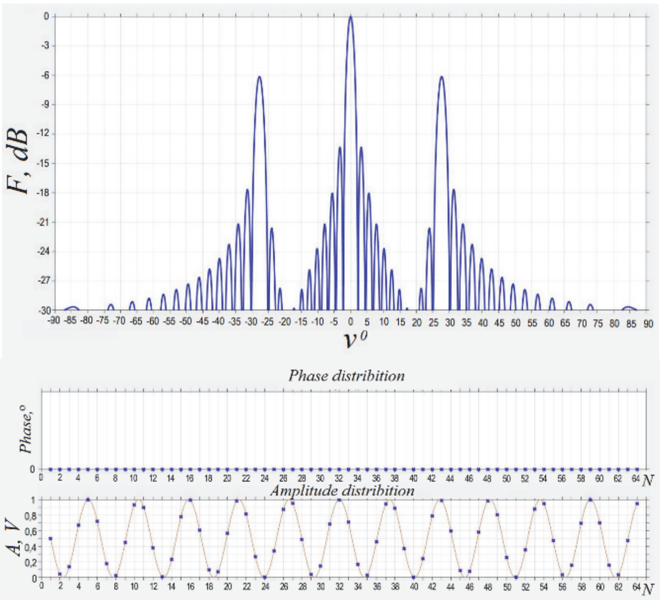

Fig. 2. Amplitude-phase distribution of the antenna array

A sinusoid with a frequency f_{sp} is shown in Fig. 2 and 3 in brown. The considered simplest synthesis methods and more complex methods described, for example, in [17-19] with modification [20] are considered direct since the solution is written as a finite sum. When considering an antenna array with a more complex configuration, they try to reduce the problem to a linear or flat array. For example, when considering ring antenna arrays, the equivalent linear radiator method is used [21-25].

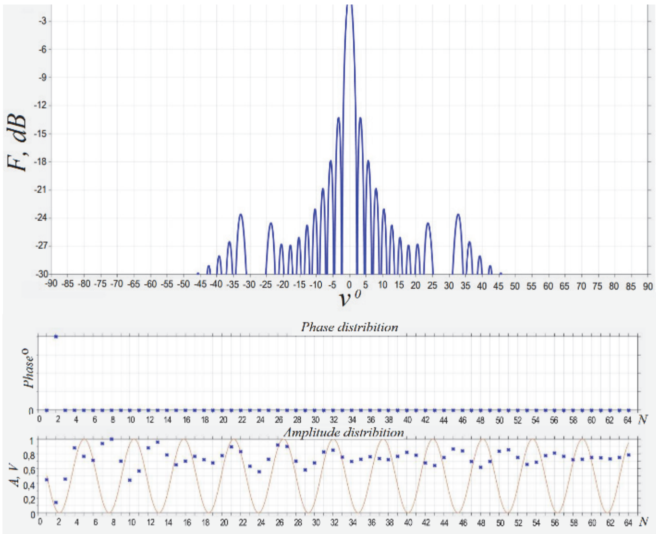

Fig. 3. Amplitude-phase distribution of the antenna array (when using a Butterworth filter)

The relationship between the angle (position of the spatial-spectral component) and the frequency of the sinusoid of spatial readings on the aperture is given by:

$$f_{sp} = \frac{\sin \upsilon}{\lambda}. \tag{3}$$

Modern approaches to the design and construction of antennas are based on structural-parametric synthesis [26-30]. These approaches are reduced to finding the geometric dimensions of the antenna using optimization methods. First, the structure of the antenna is determined, and then the values of the parameters of its elements are found. The synthesis is carried out using both analytical and numerical methods implemented in a computer-aided design system. As a result, an antenna array design is obtained, the elements of which provide good matching in the frequency band, taking into account diffraction from neighboring radiators and structural elements. Modern computing tools make it possible to carry out calculations for electrically large arrays and obtain partial radiation patterns for each radiating element.

III. Results

In an antenna array with an arbitrary arrangement of radiating elements, it is possible to select the array factor only in the first approximation. When taking into account the mutual influence, the partial radiation patterns of all antenna elements for a given direction are different. Moreover, in each angular direction, it is necessary to take into account not only the amplitude but also the phase radiation patterns. It is the partial radiation patterns that begin to play a key role in the formation of antenna array radiation patterns.

As a result of the analysis of methods for synthesizing radiation patterns to find the required amplitude-phase distribution in an antenna array with an arbitrary arrangement of radiating elements, a technique based on partial radiation patterns is proposed, which contains 4 stages.

Stage 1. For each radiating element of the antenna array, the electric field in the far zone is found in the spherical coordinate system (r, ϑ, φ). The solution is sought for a radiating element in the array, provided that the remaining radiating elements are loaded with matched loads. That is, the result is a set of 3-dimensional partial radiation patterns. It is necessary to save the results in such a way that all antennas have a single phase reference point.

Stage 2. As a result of adding the fields obtained in the first stage, each of which is preliminarily multiplied by a weighting factor (complex number), the total radiation pattern of the antenna array is obtained. The set of weight coefficients is the required amplitude-phase distribution.

Stage 3. The criterion for optimization is set. For example, maximizing the directional factor in a given direction (ϑ, φ) of a spherical coordinate system.

Stage 4. When optimizing by the particle swarm method, the amplitude-phase distribution is searched until the criterion from stage 3 of the methodology is met with a given accuracy.

The technique can be applied both at one frequency and at several at once. In addition, the phase weights found for one frequency can be translated into delays in the time domain.

Let us give some examples of the use of the proposed method. A low-profile combined ring concentric antenna array, described in detail in [31], is shown in Fig. 4 and consists of two ring arrays. The internal one operates at a center frequency of 5.0 *GHz*, and the external one operates at 2.5 *GHz*.

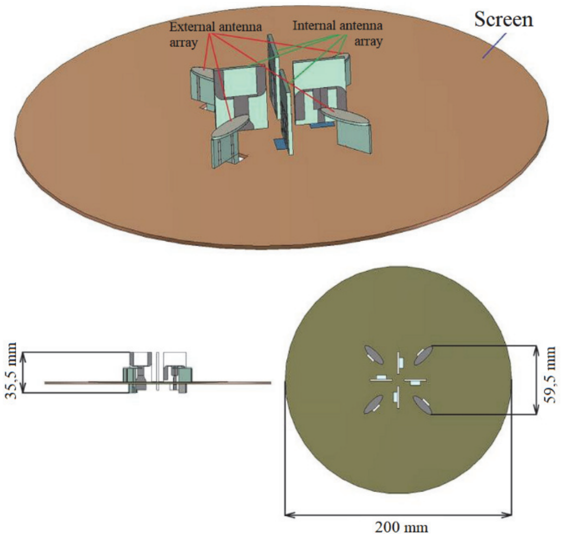

Fig. 4. Low profile combined ring concentric antenna array

We will look for the amplitude-phase distribution for the antenna shown in Fig. 1 at a frequency of 2.7 *GHz* (external radiators are involved), such that in a given direction (ϑ, φ) the directional coefficient is maximum. Take the amplitude values from 0 to 1.0 *V* in 0.1 *V* steps, and the phase from 0° to 360° in 11.25° steps. In total, each channel can have 363 weight values. Since there are 4 channels, the number of possible combinations is 363^4, or 17363069361 variants of the amplitude-phase distribution.

To illustrate the conditions of the problem and the binding of the coordinate system, Fig. 5 shows the radiation pattern of one element of the antenna array, located in the direction of 45° along φ, against the background of the array. All other radiators are loaded with matched loads. In fact, a partial radiation pattern of the emitter is shown. Here and below, the results are obtained in the computer-aided design system by the method of finite differences in the time domain.

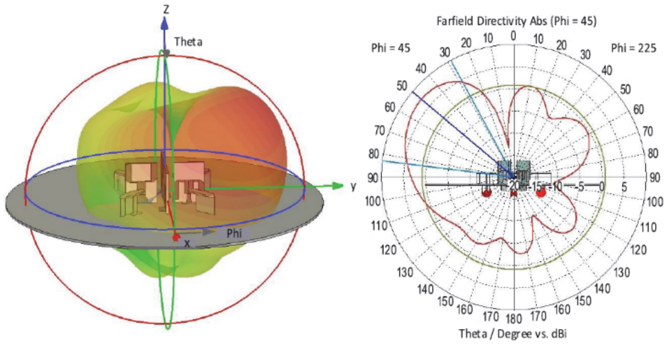

Fig. 5. Antenna system radiation patterns at $\vartheta_{\max}$=50°, $\varphi_{\max}$=45°, *DF*=7.3 *dB*

The basic steps of the algorithm used to get results in MATLAB are as follows.

Step 1. Read five electric partial fields from text files.

Step 2. Form a set of possible values of the amplitude and phase of the signal in the channel in the form of an array of complex numbers:

$$SIi = (SIi_1, SIi_2,\ldots,SIi_w,\ldots,SIi_W),$$

where W is the number of possible weight coefficients in each channel.

Step 3. Create a helper function.

Input data:

- fields obtained at step 1;
- initial data, depending on the criterion optimality (for example, the direction of the maximum radiation patterns);
- variable Q to determine the amplitude-phase distribution (necessary to simplify the application of the particle's warm optimization function and can vary from 1 to W^N; i.e. only one number is transmitted by which the amplitude-phase distribution for the channels is restored).

$$Ii_n = SIi_{pn}, \tag{4}$$

where Ii = ($Ii1$, $Ii2$,…,Iin,…,IiN) is the amplitude-phase distribution; N is the number of emitters in the antenna array;

$$p_n = ceil\left(\frac{Q}{W^{N-n}}\right) - \left(ceil\left(\frac{Q}{W^{N-n+1}}\right) - 1\right)\cdot W, \tag{5}$$

where *ceil* - MATLAB function that returns the value rounded to the nearest integer greater than the argument.

The presented algorithm allows not only finds a solution for an antenna array with no more than five radiating elements but also helps to illustrate the dependence of the objective function on the parameter. Fig. 6 shows the dependence of the coefficient of directional action in a given direction on Q, i.e., on various amplitude-phase distributions. Q changes from 1 to 17363069361 in steps 10^6 (a) and 10^7 (b). Next, we will use the described method and try to increase the directional coefficient in the direction $\varphi = 45^\circ, \vartheta = 50^\circ$ by using all emitters. As a result, we obtain the following amplitude distribution in Volts (0.4; 0.9; 0.3; 0.2) and phase distribution in degrees (−67.50; −168.75; −101.25; 45.00). In this case, $\phi_{\max} = 52^\circ, \vartheta_{\max} = 51^\circ, DF = 9.2$ dB.

In the direction, $\varphi = 45^\circ, \vartheta = 50^\circ$ the directional factor will increase compared to the directional factor of one element up to 9.15 *dB*.

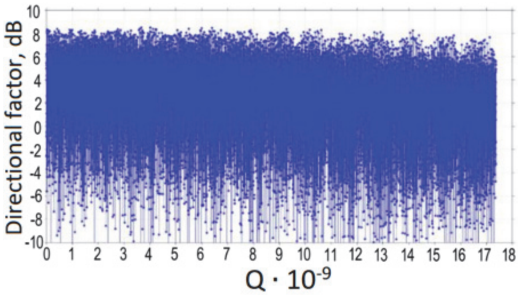

(a)

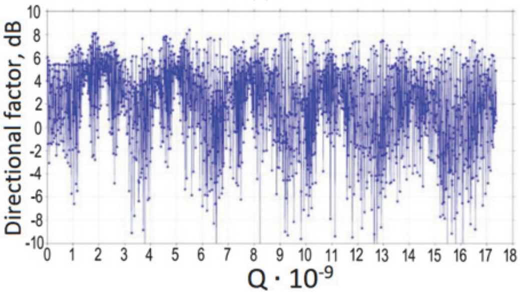

(b)

Fig. 6. The dependence of the coefficient of directional action on Q with a step: (a) 10^6; (b) 10^7

Next, we rotate the radiation patterns in φ by 90°, and leave ϑ the same, equal to 50°. We obtain the amplitude distribution (0,2; 0,7; 0,7; 0,2), and the phase distribution (11.25; –123.75; –123.75; 11.25). Fig. 7 shows the amplitude-phase distribution of the radiation patterns obtained for this. A five-element antenna array based on asymmetric "wave channel" antennas [31] is shown in Fig. 8.

The center frequency of the five-element antenna array is 2.5 GHz. Typically, such antennas are used not as arrays, but as a set of switchable antennas. If, for example, each of the antennas is connected to its receiver, then it becomes possible to work independently with several subscribers or adapt to the interference environment by choosing the antenna. Let us consider the potential possibility of joint processing of signals to form a zero in an arbitrary given direction while maintaining the direction of the maximum of the radiation patterns.

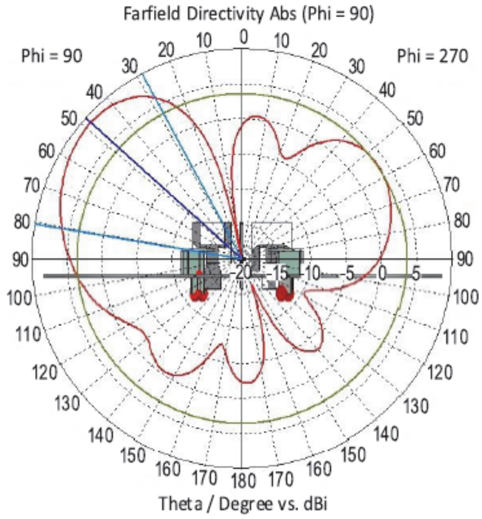

Fig. 7. Antenna array radiation patterns: $\vartheta_{\max} = 48^o$, $\varphi_{\max} = 90^o$, DF=9.0 dB

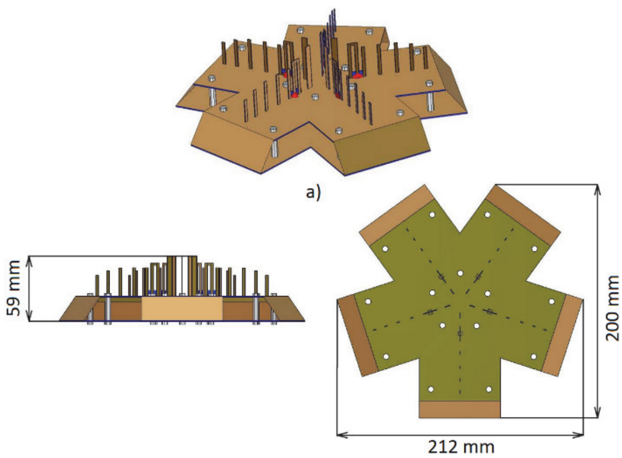

Fig. 8. Five-element antenna array based on asymmetric "wave channel" antennas

Fig. 9 shows a partial radiation pattern of an antenna array element located in the direction -18° of φ, against the background of the grating. It also shows the location of the coordinate system and the excitation ports. Coefficient of directional action at maximum ($DF_{\max}$), equal to 6.2 dB, in the screen plane $DF_{\max}|\vartheta = 90^o = 6.2$ dB.

Let's use the above algorithm and find the amplitude-phase distribution for the formation of radiation patterns in the screen plane ($\vartheta = 0^o$) with a maximum $\varphi_{\max} = 0^o$.

The direction of the zero of the radiation patterns $\varphi_{\min}$ will be changed. The optimality criterion is the maximization of the ratio of the coefficient of directional action in the direction $\varphi_{\max}$ to the coefficient of directional action at the minimum $\varphi_{\min}$. Fig. 10 shows the radiation patterns corresponding to the amplitude-phase distribution. For an antenna array with more than 5 radiating elements, we use the code for the genetic algorithm from [32-34] instead of the particle swarm method. Let's place the eight PIFA antennas as shown in Fig. 11. The amplitude distribution numbers correspond to the port numbers.

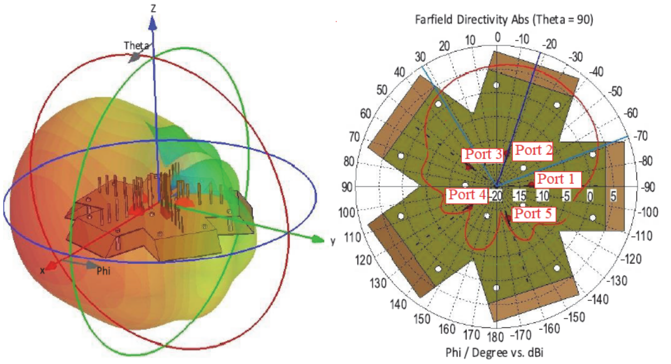

Fig. 9. The radiation patterns of the radiating element of the antenna array

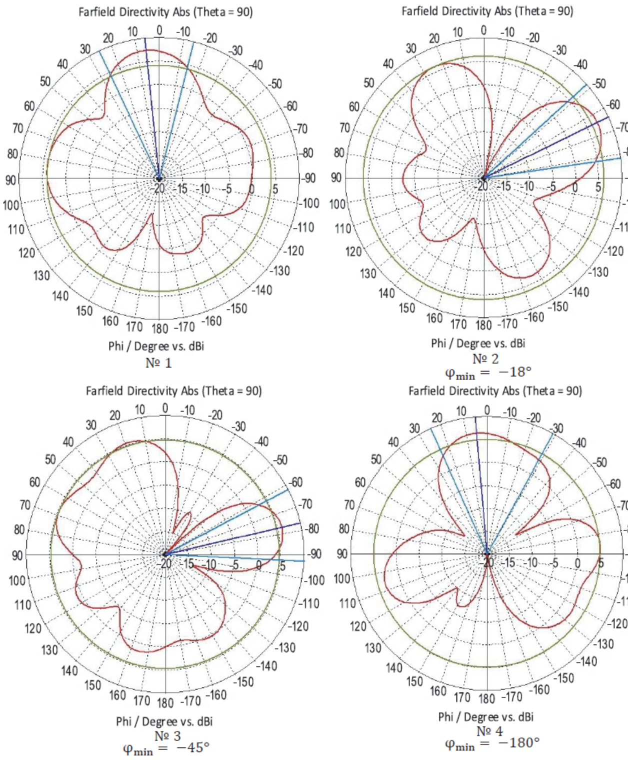

Fig. 10. Radiation patterns correspond to the amplitude-phase distribution

Let us form at a frequency of 2.7 GHz the total radiation pattern with the maximum directivity in the direction $\vartheta = 45^o$, $\varphi = -150^o$; this radiation pattern is shown in Fig. 12.

Fig. 14 shows the radiation pattern in the plane of the screen. Further, in addition to the maximum directivity coefficient in the direction $\vartheta = 45^o$, $\varphi = -150^o$, we require zero in the radiation patterns in the plane of the screen ($\vartheta = 90^o$, $\varphi = -90^o$). We will, as before, maximize the ratio of the coefficient of directional action. The results are shown in Fig. 13. The maximum of the directivity factor, equal to 9.5 dB, is shifted and obtained in the direction $\vartheta_{max} = 51^o$, $\varphi_{max} = -140^o$. Fig. 14 compares the radiation patterns shown in Fig. 12 and 13 in the plane of the screen ($\vartheta = 90^o$, $\varphi = -90^o$). The results obtained take into account all the features, both directly design antennas and carrier design.

There is no need to allocate space for a pre-designed antenna array with any known regular structure.

As shown in Fig. 11, the antenna is inscribed in the design of the carrier, which significantly reduces the weight and size. In some cases, for example, when using additive technologies, the antenna (or its elements) and the carrier can be created in a single technological cycle, which increases serial suitability and reduces the cost of the product.

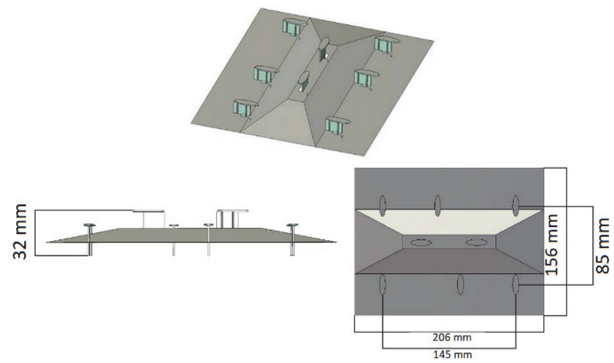

Fig. 11. Test conformal antenna array with imitation of the location of radiating elements on the carrier

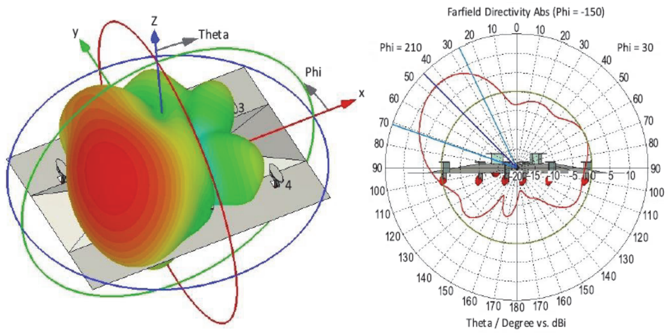

Fig. 12. Radiation patterns of a test conformal antenna array with a maximum directivity in the direction of $\vartheta = 45^o$, $\varphi = -150^o$ and its cross section at $\varphi = -150^o$

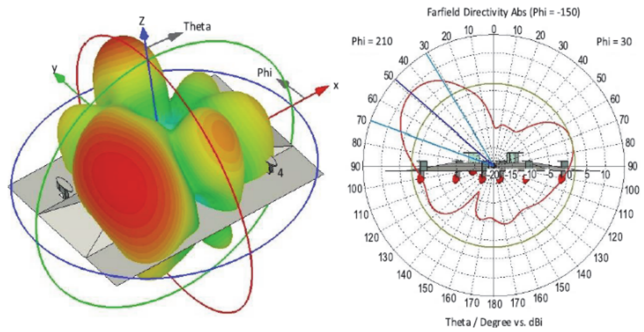

Fig. 13. Radiation patterns of a test conformal antenna array with a maximum directivity in the direction of $\vartheta = 51^o$, $\varphi = -140^o$ and its cross section at $\varphi = -150^o$

Depending on the location of the antenna and the model of external influencing factors, the design of the final product is supplemented with a radio-transparent radome or a radio-transparent shelter. Restrictions are imposed on the structural elements of such structures to protect antenna arrays due to the fact that partial radiation patterns must experience minimal and identical distortions. The proposed method allows for removing a number of limitations. For example, fairings can be of arbitrary shape and complemented by asymmetrical stiffeners.

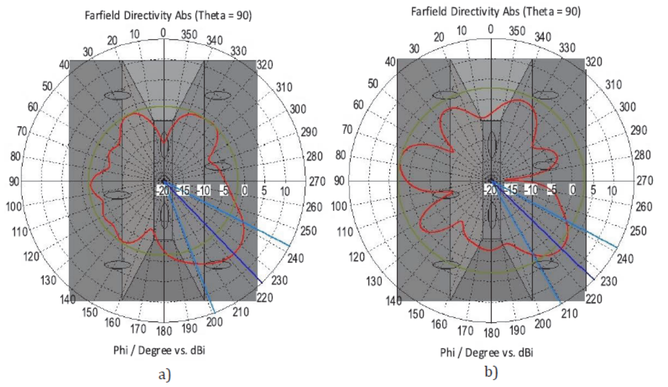

Fig. 14. Diagram of the directivity of the test conformal antenna array in the plane of the screen 11 ϑ^o φ^o $\vartheta = 90^o$, $\varphi = -90^o$, obtained by maximizing: a) in the direction $\vartheta = 45^o$, $\varphi = -150^o$; b) the ratio of the directional factor in direction $\vartheta = 45^o$, $\varphi = -150^o$ to the directional factor in direction $\vartheta = 90^o$, $\varphi = -90^o$

When analyzing and synthesizing the radiation patterns of antenna arrays with an arbitrary arrangement of radiating elements, MATLAB and Ansys HFSS software packages were used. With the help of HFSS, the optimization of the geometry of a five-element antenna array based on asymmetric "wave channel" antennas was carried out for a given objective function, which includes the characteristics of the antenna. The use of HFSS makes it possible to find the required amplitude-phase distribution two times less than other existing methods. The choice of software actually comes down to finding a compromise between the calculation speed, available computing resources, and the size of the task (size in units of wavelengths). All this comes down to solving the problem of optimizing the process of designing a five-element antenna array.

IV. Conclusion

The proposed technique makes it possible to find the required amplitude-phase distribution in a relatively short time (seconds). The algorithm constructed to obtain the results is not optimal in terms of speed and can be improved. Increasing the speed of calculations is possible with the use of specialized hardware. When solving the adaptation problem, criteria are established that are related to the signal, and not to the radiation patterns of the antenna array. For example, the minimum RMS error when compared to a reference signal. As a result, the optimal vector of weight coefficients is found, including using evolutionary optimization algorithms. This vector corresponds to a radiation pattern of a certain shape. With the help of the proposed technique, it is possible to evaluate the potential capabilities of the antenna during adaptation, taking into account mutual connections. For example, the simulation method. The technique assumes a fixed position of the radiating elements, but it can be applied to the design of reconfigurable antenna arrays.

Acknowledgment

The authors would like to thank the students and faculty of the Department of Radio Engineering and Telecommunications and the Department of Radio Electronic and Aerospace Systems of the Azerbaijan Technical University for their valuable assistance in carrying out this work, and would also like to thank them for the installation of antenna arrays, for their work on data collection and to edit the article.

References

[1] E. M. Bakkali, M. A. Ennasar, and R. F. García, "Design and Experimental Validation of a Multifunction Single Layer UHF-RFID Tag Antenna," *Advanced Electromagnetics*, vol. 11(1), pp. 22–29, 2022.

[2] I. J. Islamov, "General Approaches to Solving Problems of Analysis and Synthesis of Directional Properties of Antenna Arrays," *Advanced Electromagnetics*, vol. 11(4), pp. 22–33, 2022.

[3] S. Piltyay, "Square Waveguide Polarizer with Diagonally Located Irises for Ka-Band Antenna Systems," *Advanced Electromagnetics*, vol. 10(3), pp. 31–38, 2021.

[4] O. J. Famoriji, and T. Shongwe, "An Effective Antenna Array Diagnosis Method via Multivalued Neural Network Inverse Modeling Approach," *Advanced Electromagnetics*, vol. 10(3), pp. 58–70, 2021.

[5] A. R. Parvathy, V. G. Ajay, and M. Thomaskutty, "Circularly Polarized Split Ring Resonator Loaded Slot Antenna" *Advanced Electromagnetics*, vol. 7(5), pp. 1–6, 2018.

[6] S. Datta, K. Kar, M. Pal, and R. Ghatak, "Fractal Shaped Antenna based triband Energy Harvester," *Advanced Electromagnetics*, 6(4), pp. 22–26, 2017.

[7] I. J. Islamov, E. G. Ismibayli, M. H. Hasanov, Y. G. Gaziyev, S. R. Ahmadova, and R. Sh. Abdullayev, "Calculation of the Electromagnetic Field of a Rectangular Waveguide with Chiral Medium," *Progress in Electromagnetics Research*, vol. 84, pp. 97–114, 2019.

[8] I. J. Islamov, E. Z. Hunbataliyev, and A. E. Zulfugarli, "Numerical Simulation of Characteristics of Propagation of Symmetric Waves in Microwave Circular Shielded Waveguide with a Radially Inhomogeneous Dielectric Filling," *International Journal of Microwave and Wireless Technologies*, vol. 14, no. 6, pp. 761–767, 2021.

[9] I. J. Islamov, M. H. Hasanov, and M. H. Abbasov, "Simulation of Electrodynamic Processes in a Cylindrical-Rectangular Microwave Waveguide Systems Transmitting Information", *11th International Conference on Theory and Application of Soft Computing, Computing with Words, Perception and Artificial Intelligence, ICSCCW – 2021*, vol. 362, pp. 246–253, 2021.

[10] E. Zhou, Y. Cheng, F. Chen, H. Luo, and X. Li, "Low-Profile High-Gain Wideband Multi-Resonance Microstrip-Fed Slot Antenna with Anisotropic Metasurface," *Progress in Electromagnetics Research*, vol. 175, pp. 91–104, 2022.

[11] R. Chowdhury, and R. K. Chaudhary, "Investigation of New Sectored Hemispherical Dielectric Resonator Antennas Operating at TM101 and TE111 Mode for Circular Polarization," *Progress in Electromagnetics Research*, vol. 167, pp. 95–109, 2020.

[12] X.-T. Yuan, W. He, K.-D. Hong, C.-Z. Han, Z. Chen, and T. Yuan, "Ultra-Wideband MIMO Antenna System with High Element-Isolation for 5G Smartphone Application," *IEEE Access*, vol. 8, pp. 56281–56289, 2020.

[13] A. Zhao, and Z. Ren, "Size Reduction of Self-Isolated MIMO Antenna System for 5G Mobile Phone Applications," *IEEE Antennas Wireless Propagation Letters*, vol. 18, no. 1, pp. 152–156, 2019.

[14] K.-L. Wong, J.-Y. Lu, L.-Y. Chen, W.-Y. Li, and Y.-L. Ban, "8-Antenna and 16-Antenna Arrays Using the Quad-Antenna Linear Array as a Building Block for the 3.5-GHz LTE MIMO Operation in the Smartphone," *Microw. Opt. Technol. Lett.*, vol. 58, no. 1, pp. 174–181, 2016.

[15] M.-Y. Li, Z.-Q. Xu, Y.-L. Ban, C.-Y.-D. Sim, and Z.-F. Yu, "Eight-Port Orthogonally Dual-Polarised MIMO Antennas Using Loop Structures for 5G Smartphone," *IET Microw. Antennas Propag.*, vol. 11, no. 12, pp. 1810–1816, 2017.

[16] M. Ikram, N. Nguyen-Trong, and A. M. Abbosh, "Common-Aperture Sub-6 GHz and Millimeter-Wave 5G Antenna System," *IEEE Access*, vol. 8, pp. 199415–199423, 2020.

[17] W. Hong, "Solving the 5G Mobile Antenna Puzzle: Assessing Future Directions for the 5G Mobile Antenna Paradigm Shift," *IEEE Microw. Mag.*, vol. 18, no. 7, pp. 86–102, 2017.

[18] J. Lan, Z. Yu, J. Zhou, and W. Hong, "An Aperture-Sharing Array for 3.5/28 GHz Terminals with Steerable Beam in Millimeter Wave Band," *IEEE Trans. Antennas Propagation*, vol. 68, no. 5, pp. 4114–4119, 2020.

[19] C. Yu, S. Yang, Y. Chen, W. Wang, L. Zhang, B. Li, and L. Wang, "A Super-Wideband and High Isolation MIMO Antenna System Using a Windmill-Shaped Decoupling Structure," *IEEE Access*, vol. 8, pp. 115767–115777, 2020.

[20] R. Chandel, A. K. Gautam, and K. Rambabu, "Tapered Fed Compact UWB MIMO-Diversity Antenna with Dual Band-Notched Characteristics," *IEEE Trans. Antennas Propaation*, vol. 66, no. 4, pp. 1677–1684, 2018.

[21] X. Zhao, S. P. Yeo, and L. C. Ong, "Planar UWB MIMO Antenna with Pattern Diversity and Isolation Improvement for Mobile Platform Based on the Theory of Characteristic Modes," *IEEE Trans. Antennas Propagation*, vol. 66, no. 1, pp. 420–425, 2018.

[22] C.-Y. Wu, H. Li, J. V. Kerrebrouck, A. Vandierendonck, I. L. de Paula, L. Breyne, and O. Caytan, "Distributed Antenna System Using Sigma-Delta Intermediate-Frequency-Over-Fiber for Frequency Bands Above 24 GHz," *Journal of Lightwave Technology*, vol. 38, Issue 10, 15, pp. 2765–2773, 2020.

[23] Q. Van den Brande, S. Lemey, J. Vanfleteren, and H. Rogier, "Highly Efficient Impulse-Radio Ultra-Wideband Cavity-Backed Slot Antenna in Stacked Air-Filled Substrate Integrated Waveguide Technology," *IEEE Trans. Antennas Propag.*, vol. 66, no. 5, pp. pp. 2199–2209, 2018.

[24] M. Zada, I. A. Shah, A. Basir, and H. Yoo, "Ultra-Compact Implantable Antenna with Enhanced Performance for Leadless Cardiac Pacemaker System," *IEEE Transactions on Antennas and Propagation*, vol. 69, Issue 2, pp. 1152–1157, 2021.

[25] M. Zada, and H. Yoo, "A Miniaturized Triple-Band Implantable Antenna System for Bio-Telemetry Applications," *IEEE Trans. Antennas Propag.*, vol. 66, no. 12, pp. 7378–7382, 2018.

[26] I. A. Shah, M. Zada, and H. Yoo, "Design and Analysis of a Compact-Sized Multiband Spiral-Shaped Implantable Antenna for Scalp Implantable and Leadless Pacemaker Systems," *IEEE Trans. Antennas Propag.*, vol. 67, no. 6, pp. 4230–4234, 2019.

[27] A. Basir, and H. Yoo, "A Stable Impedance-Matched Ultrawideband Antenna System Mitigating Detuning Effects for Multiple Biotelemetric Applications," *IEEE Trans. Antennas Propag.*, vol. 67, no. 5, pp. 3416–3421, 2019.

[28] N. Hussain, M.-J. Jeong, A. Abbas, and N. Kim, "Metasurface-Based Single-Layer Wideband Circularly Polarized MIMO Antenna for 5G Millimeter-Wave Systems," *IEEE Access*, vol. 8, pp. 130293–130304, 2020.

[29] J. Kim, S. C. Song, H. Shin, and Y. B. Park, "Radiation from a Millimeter-Wave Rectangular Waveguide Slot Array Antenna Enclosed by a Von Karman Radome," *J. Electromagn. Eng. Sci.*, vol. 18, no. 3, pp. 154–159, 2018.

[30] H. Wong, Q. Wei Lin, H. Wah Lai, and X. Yin Zhang, "Substrate Integrated Meandering Probe-Fed Patch Antennas for Wideband Wireless Devices," *IEEE Trans. Compon. Packag. Manuf. Technol.*, vol. 5, no. 3, pp. 381–388, 2015.

[31] M. J. Jeong, N. Hussain, J. W. Park, S. G. Park, S. Y. Rhee, and N. Kim, "Millimeter-Wave Microstrip Patch Antenna Using Vertically Coupled Split Ring Metaplate for Gain Enhancement," *Microw. Opt. Technol. Lett.*, vol. 6, no. 10, pp. 2360–2365, 2019.

[32] W. E. I. Liu, Z. N. Chen, and X. Qing, "Broadband Low-Profile L-Probe Fed Metasurface Antenna with TM Leaky Wave and TE Surface Wave Resonances," *IEEE Trans. Antennas Propag.*, vol. 68, no. 3, pp. 1348–1355, 2020.

[33] S. F. Jilani, and A. Alomainy, "Millimetre-Wave T-Shaped MIMO Antenna with Defected Ground Structures for 5G Cellular Networks," *IET Microw. Antennas Propag.*, vol. 12, no. 5, pp. 672–677, 2018.

[34] A. Dadgarpour, M. Sharifi Sorkherizi, and A. A. Kishk, "High-Efficient Circularly Polarized Magnetoelectric Dipole Antenna for 5G Applications Using Dual-Polarized Split-Ring Resonator Lens," *IEEE Trans. Antennas Propagation*, vol. 65, no. 8, pp. 4263–4267, 2017.